

Design of High Birefringence and Low-Loss Index-Guiding Photonic Crystal Fiber by Modified Elliptical Air Holes in Fiber Cladding

Chiung-Chou Liao

Abstract—In this study, author numerically proposed a high-birefringence and low-loss index-guiding photonic crystal fiber (PCF) and compare it with three other types of PCF. Four cases of PCFs are investigated by the finite element method. A high modal birefringence is obtained when the cladding is composed of elliptical air holes placed asymmetrically, with two half-size elliptical air holes on the top and bottom of the PCF core. The size control of these air holes is the key to reaching a high birefringence and a low confinement loss. Numerical results confirm that the proposed structure at an excitation wavelength $\lambda = 1550$ nm shows a birefringence of up to 2.085×10^{-2} and a confinement loss of less than 1.63×10^{-5} dB/km.

Index Terms—Birefringence, Photonic crystal fiber, fiber cladding, air holes.

I. INTRODUCTION

PHOTONIC crystal fibers (PCFs) with air holes down their length have attracted much attention owing to the many possibilities and promising applications in communication and sensors [1-9]. When control over the polarization of light is crucial, a high birefringence (up to about 5×10^{-4}) is introduced using a number of conventional fiber techniques [10], this high birefringence reduces the coupling between the modes of degeneration. Recent studies have indicated that PCFs with a preferred direction in their geometry could exhibit a birefringence of about one order of magnitude (10^{-3} [5]) higher than those obtained with conventional techniques (10^{-4} [10]).

In this study, a novel high-birefringence index-guiding PCF is investigated using the finite element method (FEM). The proposed PCF is composed of a solid silica core surrounded by two reduced elliptical air holes on the top and bottom of the PCF core and one cladding consisting of modified elliptical air holes. Four cases of PCFs are investigated and compared in this study. The origin of the birefringence is discussed in detail and its dependences on structural parameters are analyzed. Furthermore, the effect of confinement loss is also discussed.

Manuscript received December 7, 2011. This work was supported in part by the National Science Council, Taiwan, ROC, under Grant numbers NSC 99-2112-M-231-001-MY3, NSC-100-2120-M-002-008, and NSC-100-2632-E-231-001-MY3.

C. C. Liao is with the Electronic Engineering Department, Ching Yun University, Zhong-Li, TAIWAN (Phone: +886-3-4581196 ext. 5140; fax: +886-3-4588924; e-mail: ccliao@cyu.edu.tw).

II. SIMULATION METHOD

The numerical method used in this research is FEM. To model the infinite PCF on a two-dimensional-finite-geometry (i.e., to enclose the computational domain without affecting the numerical solution), it is necessary to use anisotropic perfectly matched layers (PMLs), which are placed in contact with the outermost boundary.

III. DESIGN AND RESULT

Four cases of PCF cores are analyzed for comparison, as shown in Figs. 1(a)-1(d). For convenience in identification, corresponding fibers are named as previous structure [conventional circular air holes PCF proposed in ref. 20, see Fig. 1(a)], case 1 [modified elliptical air holes PCF, see Fig. 1(b), case 2 [same as case 1, but air holes shift by $1/2 \Lambda x$ to the left and right sides, see Fig. 1(c)], and case 3 [same as case 1, but reduced to half of the top and bottom air holes, see Fig. 1(d)]. In all four cases, the pitches (center-to-center distance between the holes) along the x- and y-axes are Λx and Λy , respectively. The radius of circular air holes of the previous structure is r . In cases 1-3, a and b denote the half-lengths of the elliptical holes along the x (minor axis)- and y (major axis)-directions, respectively. The coefficient of $\eta = a/b$ is defined to determine the relationship between the large and small air hole sizes. The refractive index of the background silica is set to be $n = 1.45$. The effective index and birefringence of PCFs are dependent on air hole size and wavelength.

Figure 2 shows plots of effective index as a function of wavelength in the four cases of the proposed PCFs with the following parameters: $\Lambda x = \Lambda y = 1.00 \mu\text{m}$, $r = 0.4 \mu\text{m}$ in the previous circular air hole case; $\Lambda x = 1.9 \mu\text{m}$, $\Lambda y = 2.2 \mu\text{m}$, $a = 0.45 \mu\text{m}$, $b = 0.542 \mu\text{m}$, elliptical ratio (a/b) = 0.83 in cases 1-3; and ring number $N = 5$ (number of air holes enclosed in the PCF core). The background index of silica is calculated using the Sellmeier equation [11,12]. It can be seen from Fig. 2 that case 3 possesses a larger difference between the effective indices than the other three cases. In all the cases, a difference between the effective indices for different polarizations is observed and the effective index decreases with increasing wavelength. An important observation is seen in Fig. 2; the proposed case 3 structure possesses a large index difference in the wavelength range of 1.45-1.65 μm and the effective index increases with increasing wavelength by approximately 1.55 μm . This can be explained by the fact that the difference

between the effective indices of the x-axis in case 3 is larger than that of the y-axis owing to the effective area of the elliptical air holes along the x-axes (minor axes) being smaller than that of the y-axes (major axes).

To illustrate the field profile of the four PCFs, a fundamental mode with the same parameters used in Fig. 2 is shown in Figs. 3(a)-3(d), which show the different patterns of confinement light in the PCF core region. The fundamental mode is strongly bound in the high-index core region with the effective indices $n_{eff,x}$ and $n_{eff,y}$, giving a birefringence $B = |n_{eff,x} - n_{eff,y}|$. It is evident in all the cases in Fig. 3 that the

intensity of the x-polarized mode is higher than that of the y-polarized mode owing to the x-polarized states having a lower air filling fraction than the y-polarized states. This implies that the asymmetry in elliptical air hole PCFs is one of the key factors in determining the localization extent of the transverse mode. Another significant finding from Fig. 3 is that the asymmetric core shape can affect the polarization mode in elliptical air hole PCFs. For example, the field pattern in the previous structure [see Fig. 3(a)] can split fields extending far beyond the core-cladding interface. It is worth confirming whether, in the case that a large birefringence is

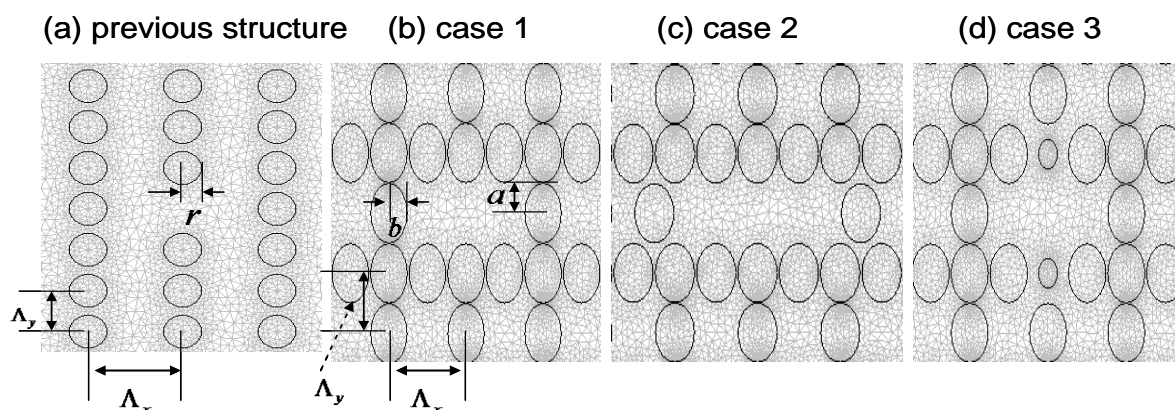


Fig 1. Cross sections in four cases of proposed PCFs.

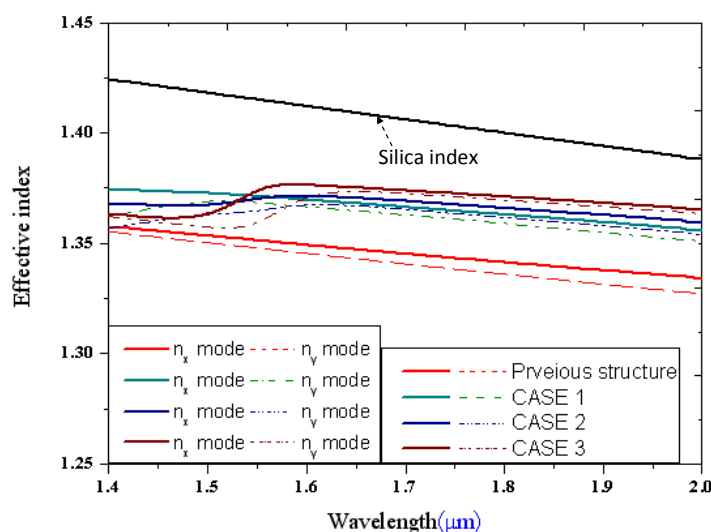


Fig. 2. Plots of effective index as a function of wavelength in four cases of PCFs with the following parameters: $\Lambda_x = \Lambda_y = 1.00\mu\text{m}$, and $r = 0.4\mu\text{m}$ for previous structure; $\Lambda_x = 1.9\mu\text{m}$, $\Lambda_y = 2.2\mu\text{m}$, $a = 0.45\mu\text{m}$, $b = 0.542\mu\text{m}$, and elliptical ratio $(a/b) = 0.83$ in cases 1-3; and ring number $N = 5$.

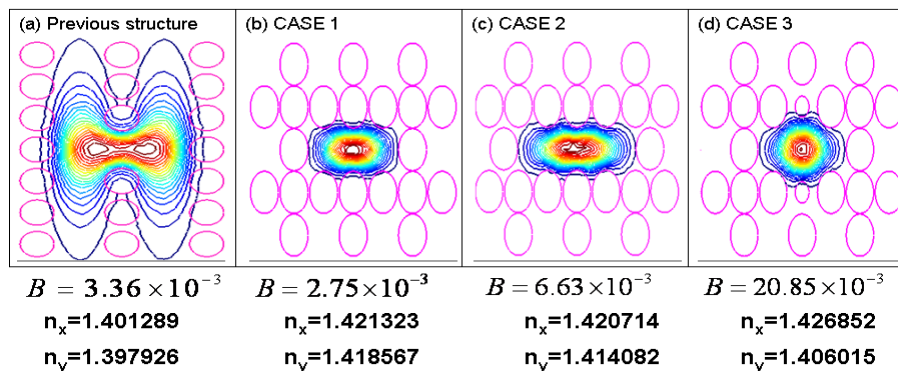


Fig. 3. Mode field patterns of four cases of PCFs.

desired, the parameters in elliptical air hole PCFs are limited by the requirement for mode profiles, which contain a higher field intensity in the core region.

Figure 4 shows plots of birefringence as a function of wavelength in the four PCFs with the same parameters used in Fig. 2. The corresponding maximum birefringences at an excitation wavelength $\lambda = 1550$ nm are as follows: in the previous case, 3.36×10^{-3} ; in case 1, 2.75×10^{-3} ; in case 2, 6.63×10^{-3} ; and in case 3, 2.085×10^{-2} . It can be clearly seen in Fig. 4 that the birefringences of the previous case and cases 1 and 2 are not sensitive to the variation in wavelength in the range of 1.4-2.0 μm . An ultrahigh birefringence is found in case 3, that is, 2.085×10^{-2} at an excitation wavelength $\lambda = 1.55 \mu\text{m}$, which is much higher than those obtained in the other cases.

The FEM with PMLs is used to calculate the confinement loss of the fundamental modes in the four cases of PCFs, and the results are plotted in Fig. 5. Figure 5 shows confinement loss as a function of wavelength in the range from $\lambda = 1.3$ to 2.0 μm with the same parameters used in Fig. 2 at an excitation

wavelength $\lambda = 1.55 \mu\text{m}$. It indicates that the confinement of the guided mode of the proposed case 3 structure is significantly improved. It can be predicted that more rings are used to achieve a low confinement loss of PCF. The confinement losses of the proposed case 1-3 structures at a wavelength of 1.55 μm are 2.674×10^{-4} dB/km in case 1, 2.025×10^{-5} dB/km in case 2, and 1.63×10^{-5} dB/km in case 3, which are much lower than that of about 1.44×10^{-2} dB/km obtained in the previous case when the number of air hole rings $N = 5$. To explain this phenomenon, the confinement field of the proposed case 3 structure is assigned to the PCF core, which is surrounded by adjacent air holes near the core and gives rise to more fields confined in the core region. It can also be observed from Figs. 3(b)-3(d) that the mode field patterns are effectively enclosed by air holes near the PCF cores. Compared with the previous structure [see Fig. 3(a)], split fields extend far beyond the core-cladding interface and a larger mode field showing leakage from the y-axis due to fewer air holes encloses the core region, which demonstrates that most of the field leakage comes from the y-direction, thus

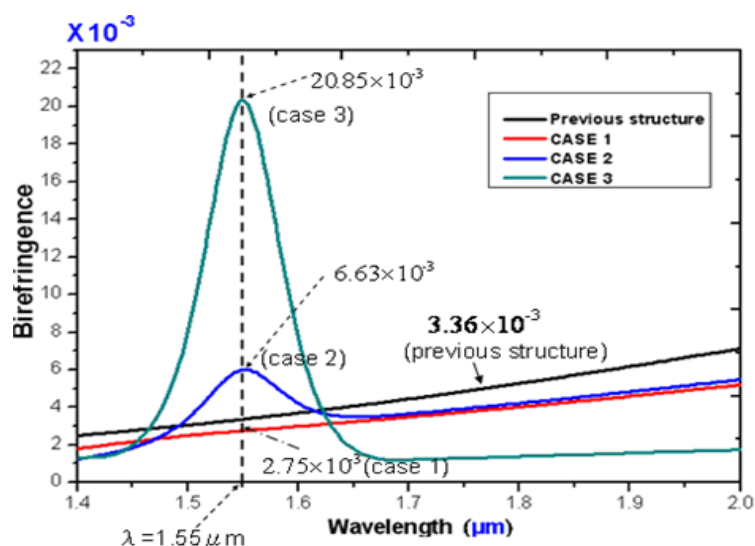


Fig. 4. Plots of birefringence as function of wavelength in the four cases of PCFs with same parameters used in Fig. 2.

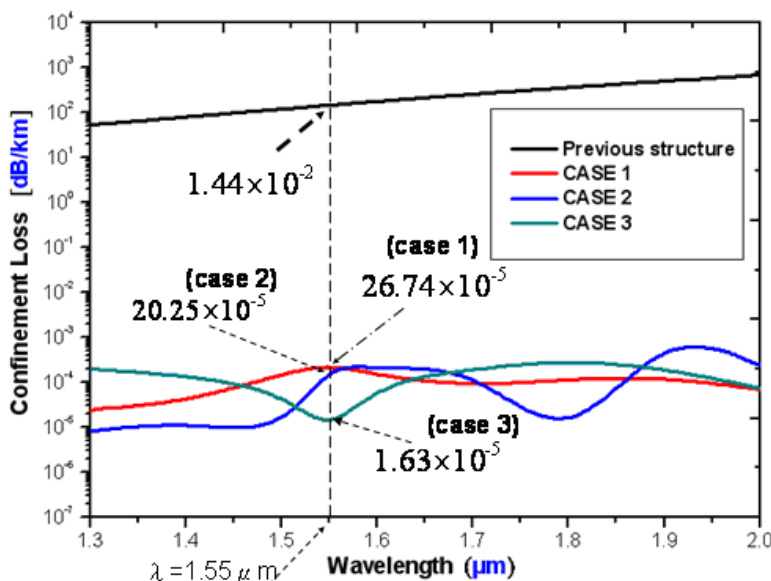


Fig. 5. Plots of confinement loss as function of wavelength in four proposed cases of PCFs, with same parameters used in Fig. 2.

resulting in a higher confinement loss.

- [16] D. Chen, M.-L. Vincent Tse, C. Wu, H. Fu, and H.-Y. Tam, "Highly Birefringent Four-Hole Fiber for Pressure Sensing," *Prog. Electromagn. Res.*, No. 114, pp. 145-158, 2011.

IV. CONCLUSIONS

High-birefringence and low-confinement-loss index-guiding elliptical air hole PCFs with a point defect enclosed by different types of air holes are successfully demonstrated. Four cases of the proposed PCFs are investigated. The birefringence of a fundamental mode and confinement loss in such a PCF are analyzed numerically using FEM. The highest modal birefringence on the order of 10⁻² and the lowest confinement loss less than 10⁻⁵ dB/km in the proposed case 3 (a cladding with modified elliptical air holes and a core of solid silica surrounded by two half-size air holes in one direction) structure at an excitation wavelength of $\lambda = 1550$ nm can be easily achieved. This result shows prospects for the development of new sensors and other optical device applications [13-16]. The merit of the designed PCFs is that their optimum birefringence and confinement loss can be easily achieved by reducing the size of two air holes near the core area.

REFERENCES

- [1] J. C. Knight, T. A. Birks, P. St. J. Russell, and D. M. Atkin, "All-silica single-mode optical fiber with photonic crystal cladding," *Opt. Lett.* No. 21, pp. 1547-1549, 1996.
- [2] P. St. J. Russell, "Photonic-Crystal Fibers," *J. Lightwave Technol.*, No. 24, pp. 4729-4749, 2006.
- [3] C. M. Jewart, S. M. Quintero, A. M. B. Braga, and K. P. Chen, "Design of a highly-birefringent microstructured photonic crystal fiber for pressure monitoring," *Opt. Express*, No. 18, pp. 25657-64, 2010.
- [4] M. Szpulak, G. Statkiewicz, J. Olszewski, T. Martynkien, W. Urbanczyk, J. Wójcik, M. Makara, J. Klimek, T. Nasilowski, F. Berghmans, and H. Thienpont, "Experimental and theoretical investigations of the birefringent holey fiber with triple defect," *Appl. Opt.*, No. 44, pp. 2652-2658, 2005.
- [5] K. Saitoh and M. Koshiba, "Photonic bandgap fibers with high birefringence," *IEEE Photonics Technol. Lett.*, No. 14, pp. 1291-1293, 2002.
- [6] Agrawal, N. Kejalakshmy, B. M. A. Rahman, and K. T. V. Grattan, "Polarization and Dispersion Properties of Elliptical Hole Golden Spiral Photonic Crystal Fiber," *Appl. Phys. B*, No. 99, pp. 717-726, 2010.
- [7] N. A. Issa, M. A. van Eijkelenborg, M. Fellew, F. Cox, G. Henry, and M. C. J. Large, "Fabrication and study of microstructured optical fibers with elliptical holes," *Opt. Lett.*, vol. 29, no. 12, pp. 1336-1338, 2004.
- [8] T. A. Birks, J. C. Knight, and P. St. J. Russell, "Endlessly single-mode photonic crystal fiber," *Opt. Lett.*, No. 22, pp. 961-963, 1997.
- [9] J. C. Knight and P. St. J. Russell, "Applied optics: new ways to guide light," *Science*, No. 296, pp. 276-277, 2002.
- [10] J. Noda, K. Okamoto, and Y. Sasaki, "Polarization-Maintaining Fibers and Their Applications," *J. Lightwave Technol.*, No. 4, pp. 1071-1089, 1986.
- [11] Y.-F. Chau, C.-Y. Liu, H.-H. Yeh, and D. P. Tsai, "A comparative study of high birefringence and low confinement loss photonic crystal fiber employing elliptical air holes in fiber cladding with tetragonal lattice", *Electromagnetic Research B*, PIERB 22, pp. 39-52, 2010.
- [12] H. Bach, and N. Neuroth, *The Properties of Optical Glass*, Springer, Heidelberg, Chap. 1, 15., 1995.
- [13] T. P. White, R. C. McPhedran, C. M. de Sterke, L. C. Botten, and M. J. Steel, "Confinement losses in microstructured optical fibers," *Opt. Lett.*, No. 26, pp.1660-1662, 2001.
- [14] Betourne, V. Pureur, G. Bouwmans, Y. Quiquempois, L. Bigot, M. Perrin, and M. Douay, "Solid photonic bandgap fiber assisted by an extra air-clad structure for low-loss operation around 1.5 μm ," *Opt. Express*, No. 15, pp. 316-324, 2007.
- [15] C. M. Jewart, S. M. Quintero, A. M. B. Braga, and K. P. Chen, "Design of a highly-birefringent microstructured photonic crystal fiber for pressure monitoring," *Opt. Express*, No. 18, pp. 25657-664, 2010.